Paper

Modeling of Ar Induction Thermal Plasma with an Injection of PTFE Powder

Chun Wang* Non-member
Yasunori Tanaka* Member
Tadahiro Sakuta

Modeling was made of Ar induction thermal plasma with an injection of PTFE powder to study fundamentally the effects of polymer ablation on thermal plasma. Interactions between thermal plasma and PTFE powder such as heat conduction, melting, evaporation and radiation was simply taken into account. At the same, the behavior of particle in the plasma was also investigated. The predicted results shows that the injection of PTFE powder can cause the local cooling of Ar thermal plasma temperature field, and that increasing powder feed-rate decreases plasma temperature around torch central axis. Moreover, it was seen that smaller powder size decays plasma much more. On the other hand, it is found that particle trajectory as well as temperature history relate to powder loading, powder size and injection location of particle. This calculated result concerning plasma temperature was compared with the experimental result.

Keywords: induction thermal plasma, interaction between plasma and particles, PTFE, modeling

1. Introduction

In the gas circuit breaker (GCB), an electric arc plasma is established between the electrodes during the current interrupting period, and is quenched by working-gas in the nozzle. The arc plasma may induce ablation of the nozzle, and is contaminated inevitably with the nozzle material. One of the nozzle materials mainly used in the GCB is PTFE (Polytetrafluoroethylene). It is therefore important to investigate the effects of soild PTFE contacting thermal plasma or arc plasma. Y. Tanaka *et al.* have been studying arc-quenching properties of various gases using an inductively coupled thermal plasma (ICTP) apparatus [(1)~(3)]. The distinguishing feature of the ICTP is to produce clean plasma without any electrode. The ICTP can be used to investigate not only the properties of pure gas plasma, but also the influence of solid or liquid material on gas plasma properties by injecting these material into the plasma fundamentally. A contact of a solid such as PTFE affects a thermal plasma in two points: one of which is ablated gas effects on thermodynamic properties of a thermal plasma, the other is an energy consumption due to melting and evaporation, which can change a temperature distribution of a thermal plasma and then its dynamic behavior. The solid contact with thermal plasmas involves various processes including phase transitions. However they are very complicated to understand in detail. Thus, numerical approach is useful for this purpose.

In the present paper, a model of Ar induction thermal plasma with PTFE powder injection was developed. Argon is the most suitable gas to produce ICTP with sufficient stability, and use of noble Ar permits us to make a fundamental investigation of ablation phenomena. This work is a first trial of the fundamental investigation on such the phenomena. This model treats two aspects of the interactions between particles and plasma: one of which is the individual particle trajectories and heating in thermal plasma, the other is the entire influence of powder melting or ablation on the thermal plasma. Using this modeling, the interactions between Ar induction thermal plasma and PTFE particles injected into the plasma were studied.

* Department of Electrical and Electronic Engineering, Kanazawa University
2-40-20, Kodatsuo, Kanazawa 920-8667

2. Modeling

A schematic of the ICTP torch geometry and its principal dimensions used is given in Fig. 1. Details of this torch were described in Ref. (1). Powder is injected from the top along the torch axis together with carrier gas.

The proposed model is based on the PSI-Cell concept developed by C.T. Crowe *et al.* [(4)], and is an extension of the work by P. Proulx and co-workers [(5)~(7)]. In this model, the mass, momentum and energy exchange rates per unit volume between the plasma and the particles are introduced as source terms in the corresponding conservation equations for the plasma and particles. Moreover the following conditions were supposed:

(1) The plasma is assumed to be in local thermodynamic equilibrium and optically thin.
(2) The flow is steady, laminar, axis-symmetric with negligible viscous dissipation.
(3) Two-dimensional electromagnetic fields are considered in present model.
(4) For injected particles, the particle-particle interactions are neglected and no internal heat

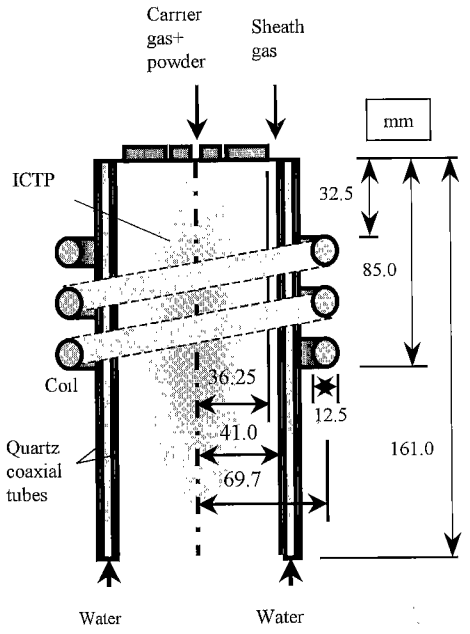

Fig. 1. Schematic diagram of ICTP

transfer in the particles is considered.

2.1 Plasma Equations On the basis of above assumptions, the plasma equations can be written as follows:

(1) Continuity:

$$\frac{\partial(\rho u)}{\partial z}+\frac{1}{r}\frac{\partial(\rho r v)}{\partial r}=S_{\mathrm{p}}{}^{C} \quad \cdots\cdots (1)$$

(2) Momentum transfer equations:

$$\rho u\frac{\partial u}{\partial z}+\rho v\frac{\partial u}{\partial r}=-\frac{\partial p}{\partial z}+2\frac{\partial}{\partial z}\left(\eta\frac{\partial u}{\partial z}\right)+\frac{1}{r}\frac{\partial}{\partial r}\left[\eta r\left(\frac{\partial u}{\partial r}+\frac{\partial v}{\partial z}\right)\right]+\mu_0\sigma\Re\left[\dot{E}_\theta\dot{H}_r^*\right]+S_{\mathrm{p}}{}^{M_z} \quad \cdots\cdots (2)$$

$$\rho u\frac{\partial v}{\partial z}+\rho v\frac{\partial v}{\partial r}=-\frac{\partial p}{\partial r}+\frac{\partial}{\partial z}\left[\eta\left(\frac{\partial v}{\partial z}+\frac{\partial u}{\partial r}\right)\right]+\frac{2}{r}\frac{\partial}{\partial r}\left[\eta r\left(\frac{\partial v}{\partial r}\right)\right]-\frac{2\eta v}{r^2}+\mu_0\sigma\Re\left[\dot{E}_\theta\dot{H}_z^*\right]+S_{\mathrm{p}}{}^{M_r} \quad \cdots\cdots (3)$$

(3) Energy transfer equation:

$$\rho u\frac{\partial h}{\partial z}+\rho v\frac{\partial h}{\partial r}=\frac{\partial}{\partial z}\left(\frac{\lambda}{C_{\mathrm{p}}}\frac{\partial h}{\partial z}\right)+\frac{1}{r}\frac{\partial}{\partial r}\left(\frac{\lambda}{C_{\mathrm{p}}}r\frac{\partial h}{\partial r}\right)+\sigma\left|\dot{E}_\theta\right|^2-P_{\mathrm{rad}}-S_{\mathrm{p}}^{E} \quad \cdots\cdots (4)$$

(4) Mass transfer equation:

$$\rho u\frac{\partial c_{\mathrm{PTFE}}}{\partial z}+\rho v\frac{\partial c_{\mathrm{PTFE}}}{\partial r}=\frac{\partial}{\partial z}\left(\rho D_{\mathrm{PTFE}}\frac{\partial c_{\mathrm{PTFE}}}{\partial z}\right)+\frac{1}{r}\frac{\partial}{\partial r}\left(\rho D_{\mathrm{PTFE}}r\frac{\partial c_{\mathrm{PTFE}}}{\partial r}\right)+S_{\mathrm{p}}^{C} \quad \cdots\cdots (5)$$

(5) Vector Potential:

$$\frac{\partial^2 A_{\mathrm{R}}}{\partial z^2}+\frac{1}{r}\frac{\partial}{\partial r}\left(r\frac{\partial A_{\mathrm{R}}}{\partial r}\right)-\frac{A_{\mathrm{R}}}{r^2}+\mu_0\sigma\omega A_{\mathrm{I}}=0 \quad \cdots\cdots (6)$$

$$\frac{\partial^2 A_{\mathrm{I}}}{\partial z^2}+\frac{1}{r}\frac{\partial}{\partial r}\left(r\frac{\partial A_{\mathrm{I}}}{\partial r}\right)-\frac{A_{\mathrm{I}}}{r^2}-\mu_0\sigma\omega A_{\mathrm{R}}=0 \quad \cdots\cdots (7)$$

$$\dot{A}_\theta=A_{\mathrm{R}}+jA_{\mathrm{I}} \quad \cdots\cdots (8)$$

$$\dot{E}_\theta=-j\omega\dot{A}_\theta \quad \cdots\cdots (9)$$

$$\mu_0\dot{H}_z=\frac{1}{r}\frac{\partial}{\partial r}\left(r\dot{A}_\theta\right) \quad \cdots\cdots (10)$$

$$\mu_0\dot{H}_r=-\frac{\partial}{\partial z}\left(\dot{A}_\theta\right) \quad \cdots\cdots (11)$$

where r: radial position; z: axial position; u: axial flow velocity; v: radial flow velocity; p: pressure; ρ: mass density; h: enthalpy; η: viscosity; λ: thermal conductivity; C_{p}: specific heat at a constant pressure; σ: electrical conductivity; The calculation method about the thermodynamic and transport properties ρ, h, η, λ, C_{p} and σ is directed in section 2.4. c_{PTFE}: mass concentration of PTFE vapor; D_{PTFE}: PTFE vapor diffusion coefficient, the calculation method of which can be referred to Ref. (8); μ_0: the permeability of vacuum; A_{R}, A_{I}: real part and imaginary part of the phasor of vector potential $\dot{A}_\theta$; $\dot{E}_\theta$: the phasor of the electric field strength; $\dot{H}_z$, $\dot{H}_r$: the phasor of axial and radial component of magnetic field strength; j: complex factor ($j^2=-1$). The magnitude of the phasors including $\dot{A}_\theta$, $\dot{E}_\theta$, $\dot{H}_z$ and $\dot{H}_r$ is defined as the root mean square value. The quantities S_{p}^{C}, $S_{\mathrm{p}}^{M_z}$, $S_{\mathrm{p}}^{M_r}$, S_{p}^{E} are the source terms produced by particles, and the calculation of which will be given in section 2.3.

2.2 Particle Equations On the assumption that forces affecting an individual particle are only drag and gravity, the momentum equations for a single particle injected vertically downwards into the plasma can be expressed as [5]:

$$\frac{du_{\mathrm{p}}}{dt}=-\frac{3}{4}C_{\mathrm{D}}(u_{\mathrm{p}}-u)U_{\mathrm{R}}\left(\frac{\rho}{\rho_{\mathrm{p}}d_{\mathrm{p}}}\right)+g \quad \cdots\cdots (12)$$

$$\frac{dv_{\mathrm{p}}}{dt}=-\frac{3}{4}C_{\mathrm{D}}(v_{\mathrm{p}}-v)U_{\mathrm{R}}\left(\frac{\rho}{\rho_{\mathrm{p}}d_{\mathrm{p}}}\right) \quad \cdots\cdots (13)$$

$$U_{\mathrm{R}}=\sqrt{(u_{\mathrm{p}}-u)^2+(v_{\mathrm{p}}-v)^2} \quad \cdots\cdots (14)$$

The particle temperature, liquid fraction and diameter are determined according the following energy balances:

$$Q=\pi {d_{\mathrm{p}}}^2 h_{\mathrm{c}}(T-T_{\mathrm{p}})-\pi {d_{\mathrm{p}}}^2\sigma_{\mathrm{s}}\varepsilon({T_{\mathrm{p}}}^4-{T_{\mathrm{a}}}^4) \quad \cdots\cdots (15)$$

$$\frac{dT_{\mathrm{p}}}{dt}=\frac{6}{\pi\rho_{\mathrm{p}}{d_{\mathrm{p}}}^3 c_{\mathrm{pp}}}Q \quad \text{for } T_{\mathrm{p}}<T_{\mathrm{m}} \text{ and } T_{\mathrm{m}}<T_{\mathrm{p}}<T_{\mathrm{b}} \quad \cdots\cdots (16)$$

$$\frac{d\chi}{dt}=\frac{6}{\pi\rho_{\mathrm{p}}{d_{\mathrm{p}}}^3 H_{\mathrm{m}}}Q \quad \text{for } T_{\mathrm{p}}=T_{\mathrm{m}} \quad \cdots\cdots (17)$$

$$\frac{dd_p}{dt} = -\frac{2}{\pi\rho_p {d_p}^2 H_v} Q \quad \text{for } T_p = T_b \cdots\cdots\cdots (18)$$

u_p, v_p: axial and radial velocity component of particle, respectively; ρ_p: particle mass density; d_p: particle diameter; Q: the net heat exchange between the particle and its surroundings; T_p, T_m and T_b: the particle temperature, melting point temperature and boiling point temperature, respectively; T: plasma temperature; ε: the particle emissivity; T_a: ambient temperature which means environmental temperature around the torch exterior; σ_s: Stefan-Boltzmann constant; c_{pp}: particle specific heat; H_m and H_v: latent heat of particle melting and that of particle boiling, respectively; χ: the liquid mass fraction of the particle; U_R: the relative speed between the particle and the plasma. The formula about drag coefficient C_D and heat transfer coefficient h_c can be found in Ref. (6).

2.3 Particle Source Terms In the philosophy of the PSI-Cell approach [4], the particles are regarded as sources of mass, momentum and energy of plasma equations.

Let N_t^0 be the total number of particles injected per unit time, n_d is the particle size distribution, and n_r represents the fraction of N_t^0 injected at each point over the torch central inlet. The total number of particles per unit time traveling along the trajectory (l, k) corresponding to a particle diameter d_l injected at the point r_k is:

$$N^{(l,k)} = n_{d_l} n_{r_k} {N_t}^0 \cdots\cdots\cdots (19)$$

The particle concentration n_r in the inlet is assumed to be uniform. For the sake of computation, the powder input position is set to five points, which are at radial positions of 0.3, 0.6, 0.9, 1.2 and 1.5 mm. In the actual experimental condition, the injected powder consists of various size particles. In the computation, we assume that the powder consists of seven discrete particles and the particle with a powder average diameter has a fraction of 60%. Table 1 shows the assumed distribution fraction of particles. The distribution fraction of the other particles was also assumed to decrease with increasing deviation of its diameter from powder average diameter. As a result, that gives rise to 35 different possible particle trajectories. The injection velocity of the particle is assumed to be equal to the velocity of carrier gas. The average diameter of powder D was obtained by the measurements.

The source term in the continuity equation, S_p^C, is the net efflux rate of particle mass in a computational cell (control volume). On the assumption that the particles are spherical, the efflux rate of particle mass due to the particle trajectory (l, k) which traverses a given cell (i, j) is:

$${S_{p,ij}}^{C(l,k)} = \frac{1}{6}\pi\rho_p N_{ij}^{(l,k)} ({d_{ij,in}}^3 - {d_{ij,out}}^3) \cdots (20)$$

The net efflux rate of particle mass is obtained by summing over all particle trajectories which traverse a given cell:

Table 1. Size distribution and fraction of powder

Diameter	Fraction
0.9D	0.03
0.933D	0.07
0.966D	0.1
D	0.6
1.033D	0.1
1.066D	0.07
1.1D	0.03

Note: D is the average diameter of powder

$${S_{p,ij}}^C = \sum_l \sum_k {S_{p,ij}}^{C(l,k)} \cdots\cdots\cdots\cdots (21)$$

The momentum source terms are evaluated in the same fashion as the particle mass source terms. In this case, the efflux rate of particle momentum due to particle trajectory (l, k) traversing a given cell (i, j) is:

$${S_{p,ij}}^{M_z(l,k)} = \frac{1}{6}\pi\rho_p N_{ij}^{(l,k)} (u_{ij,in}{d_{ij,in}}^3 - u_{ij,out}{d_{ij,out}}^3) \cdots\cdots\cdots\cdots (22)$$

$${S_{p,ij}}^{M_r(l,k)} = \frac{1}{6}\pi\rho_p N_{ij}^{(l,k)} (v_{ij,in}{d_{ij,in}}^3 - v_{ij,out}{d_{ij,out}}^3) \cdots\cdots\cdots\cdots (23)$$

and the corresponding momentum source terms are:

$${S_{p,ij}}^{M_z} = \sum_l \sum_k {S_{p,ij}}^{M_z(l,k)} \cdots\cdots\cdots\cdots (24)$$

$${S_{p,ij}}^{M_r} = \sum_l \sum_k {S_{p,ij}}^{M_r(l,k)} \cdots\cdots\cdots\cdots (25)$$

The energy source term includes the heat given to the particles $Q_{p,ij}^{(l,k)}$, and superheat to bring the particle vapors into thermal equilibrium with the plasma $Q_{v,ij}^{(l,k)}$:

$$Q_{p,ij}^{(l,k)} = \int_{\tau_{in}}^{\tau_{out}} \pi {d_p}^2 h_c [T_{ij} - T_{p,ij}^{(l,k)}] dt \cdots\cdots (26)$$

$$Q_{v,ij}^{(l,k)} = \int_{\tau_{in}}^{\tau_{out}} \frac{\pi}{2}\pi {d_p}^2 \rho_p \left(\frac{dd_p}{dt}\right) c_{pp} [T_{ij} - T_{p,ij}^{(l,k)}] dt \cdots\cdots\cdots\cdots (27)$$

$${S_{p,ij}}^E = \sum_l \sum_k N_{ij}^{(l,k)} [Q_{p,ij}^{(l,k)} + Q_{v,ij}^{(l,k)}] \cdots\cdots\cdots\cdots (28)$$

2.4 Thermo-Physical Properties First, particle compositions of Ar and PTFE vapor were calculated using minimization technique of the total Gibbs free energy of the plasma. Then the thermodynamic and transport properties of pure Ar and PTFE vapor were calculated using the first-order approximation of Chapman-Enskog method. The thermodynamic and transport properties of the mixture of Ar and PTFE vapor were estimated according to the empirical proportion combination rule [8].

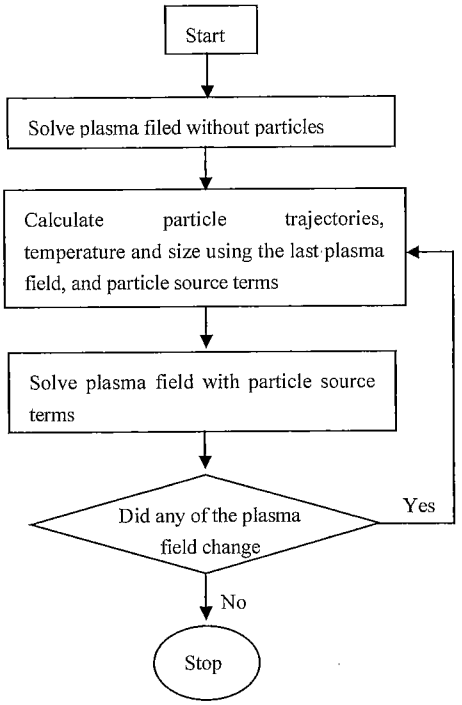

Fig. 2. Flow chart of the computational method

Table 2. Summary of the plasma operating conditions

Input power to the plasma	30 kW
Oscillator frequency	1.67 MHz
Pressure	101325 Pa
Sheath gas flow rate	Ar: 100 liters/min
Carrier gas flow rate	Ar: 6 liters/min

Table 3. Physical properties of PTFE powder [10]

Boiling point temperature (K)	895
Density (kg/m^3)	2,160
Boiling latent heats (J/kg)	1060,000
Solid specific heats (J/(kg K))	1,610
Vapor specific heats (J/(kg K))	1,610
Emissivity of particle surface	0.3

2.5 Calculation Procedure and Calculation Conditions The complete solution for a plasma-particle flow field is illustrated in Fig. 2. The calculation starts by solving the plasma flow field assuming that no powder is present. Using this flow field, individual particle trajectories together with temperature and size history along the trajectories are calculated. The mass, momentum and energy source terms for each control volume throughout the flow field then are determined. The plasma flow field is solved again incorporating these source terms. The new plasma flow field is used to establish new particle trajectories, temperature and size history and to calculate the new source terms, thereby completing the cycle of mutual interaction. Iterations are repeated for as many times as needed convergence of the plasma and the solution that accounts for the mutual interaction between powder and plasma are obtained. The SIMPLER algorithm of Patankar [9] is used for solving the above plasma flow field. In the calculation, the torch is divided into non-uniform grids of 30×34 in radial and axial direction, respectively.

A summary of the plasma operating conditions used for all the calculation in this paper is presented in Table 2. The physical properties of PTFE powder used in the present investigation are listed in Table 3 [10].

3. Interactions Between Ar Plasma and PTFE Particles for Different Powder Feed Rates

In this paragraph, attention is given to the problem of plasma-particle interactions for different powder feed-rate. For all simulations, the other conditions are kept constant, only the powder feed-rate is changed to study its effect on the overall process of thermal treatment of powder in the ICTP. Two aspects of the thermal treatment are investigated: the behavior of the individual particle, and the global effect of powder on the plasma. Computations were made for powder feed-rate of 5, 10, 20, 30 and 40 g/min, powder average diameter was fixed at 300 μm.

3.1 Individual Particle Trajectories and Temperature History Figure 3 shows the trajectories of particles initially injected at $r = 0.3$ and 1.5 mm. The corresponding temperature history as a function of the distance traveled in the axial direction is shown in Fig. 4.

The particle temperature history shows that: (i) Decreasing powder feed-rate quickens the temperature rising of the particles, which indicates powder feed-rate may affect plasma temperature, and in turn plasma temperature affects particle absorbing heat from plasma. (ii) The initial injection location of the particle influences its heating, which indicates uneven distribution of plasma radial temperature.

On the other hand, the influence of powder feed-rate on the trajectories of the particle can hardly be observed as seen in Fig. 3. Another noticeable fact is that in these calculation cases, the resultant particle temperatures do not reach to PTFE boiling temperature. This does not affect thermodynamic properties of Ar thermal plasma.

3.2 Plasma Fields As implied in the previous section, an increase in the powder feed-rate can have an important cooling effect on the temperature field in the plasma. The streamlines and isotherm contours of Ar induction thermal plasma in the absence and presence of PTFE powder are depicted in Fig. 5. The left part (a) of this figure represents the flow and temperature fields in the absence of powder, while the right part (b) corresponds to that in the presence of PTFE powder at a feed rate of 40 g/min. The tangent of streamlines indicates gas flow direction. Numerical numbers on the streamlines are values of a stream function referred to the point (0,0). As seen in Fig. 5, there is a vortex in the upper side of the torch. Because the trajectories of the particles are very close to torch central line as observed in Fig. 3, the plasma is significantly cooled down in this region due to heat absorption of particles from thermal plasma. The plasma temperature decreases from 5100 K to 2800 K at $Z = 95$ mm on the center axis with powder injection of 40 g/min. However, the outer region of the plasma remains largely unaffected by the powder

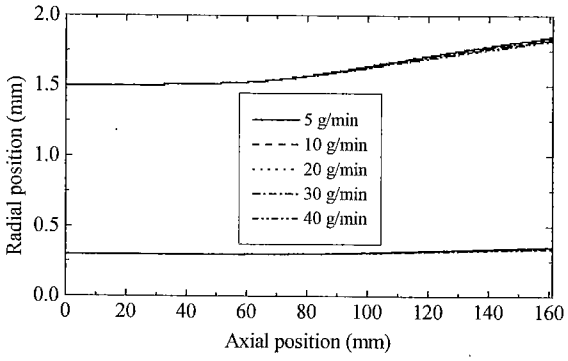

Fig. 3. Trajectories of the particles injected into plasma

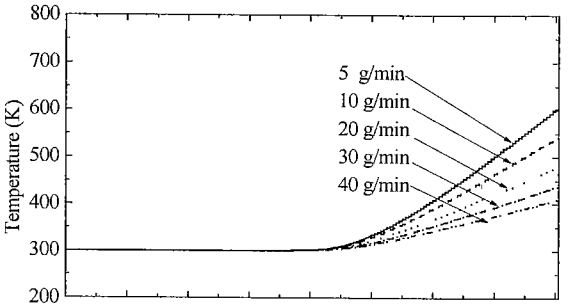

(a) Particles of initial injection at $r = 0.3$ mm

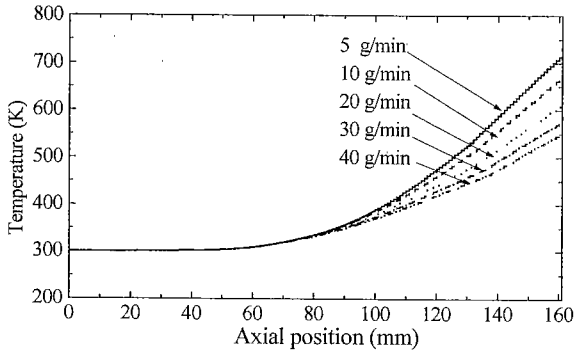

(b) Particles of initial injection at $r = 1.5$ mm

Fig. 4. Temperature history of the particles injected into plasma

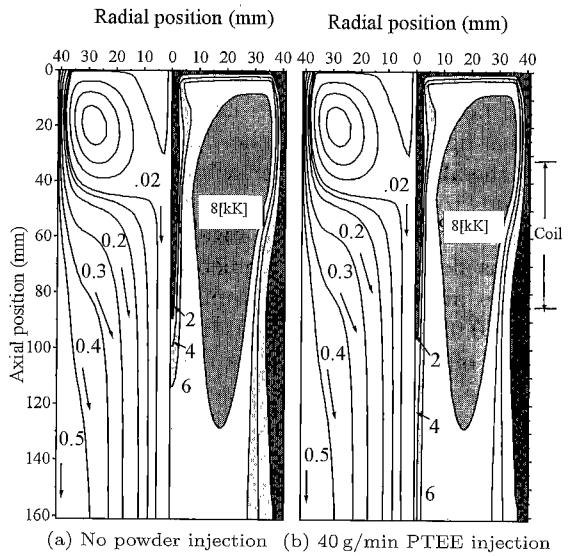

(a) No powder injection (b) 40 g/min PTEE injection

Fig. 5. Flow and temperature fields of Ar plasma

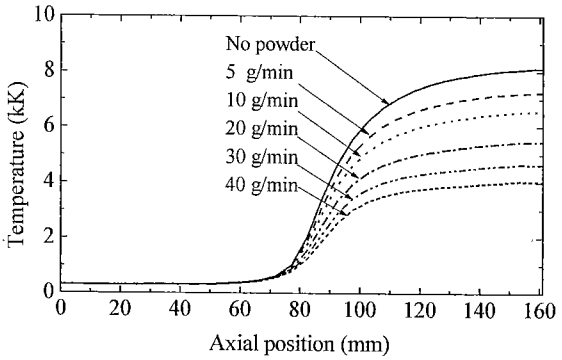

Fig. 6. Plasma temperature profiles along torch central axis

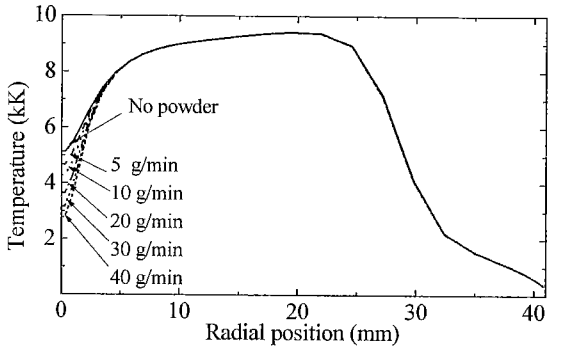

Fig. 7. Plasma temperature profiles along radial position at 10 mm below coil end

injection. The flow pattern, on the other hand, is relatively little changed by the presence of powder.

The cooling effect that an increase in powder feed-rate causes can be observed from plasma axial and radial temperature profiles shown in Figs. 6 and 7. From the two figures, we may further find that: (i) From $z = 0$ to 60 mm, plasma temperature on torch central line is not affected by the injection of powder, where the cooling is due to carrier gas. (ii) The radial limit of the influence of powder on plasma temperature is about $r = 7$ mm. The plasma temperature in the region $r > 7$ mm hardly changes as powder feed-rate.

4. Interactions between Ar Plasma and PTFE Powder for Various Powder Average Size

In this section, the effect of powder size on the interaction of plasma-particle is investigated. Computations were carried out for PTFE powder of average diameters 250–500 μm. Powder feed-rate was fixed at 5 g/min.

4.1 Individual Particle Trajectories and Temperature History Figure 8 shows the trajectories of the particles injected at two limiting injection locations of $r = 0.3$ mm and $r = 1.5$ mm for various powder sizes.

The particle trajectories show that: (i) The particles of initial injection location at $r = 0.3$ mm, regardless of particle size, move almost vertically downwards to $z = 80$ mm, then a slight drift of smaller particles can be found. (ii) For the particles injected at $r = 1.5$ mm, they begin to appear drift at $z = 30$ mm, and the

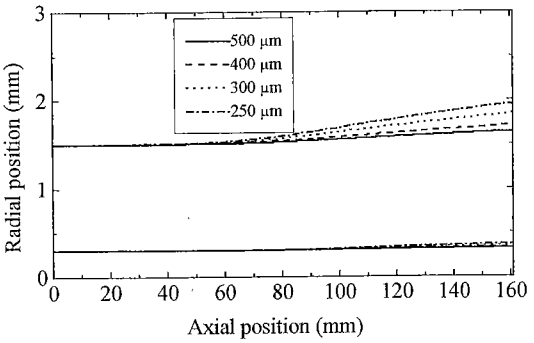

Fig. 8. Trajectories of the particles injected into plasma

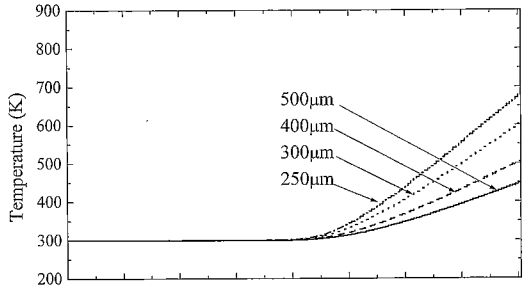

(a) Particles of initial injection at $r = 0.3$ mm

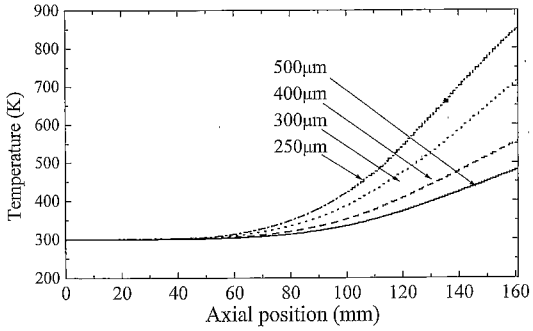

(b) Particles of initial injection at $r = 1.5$ mm

Fig. 9. Temperature history of the particles injected into plasma

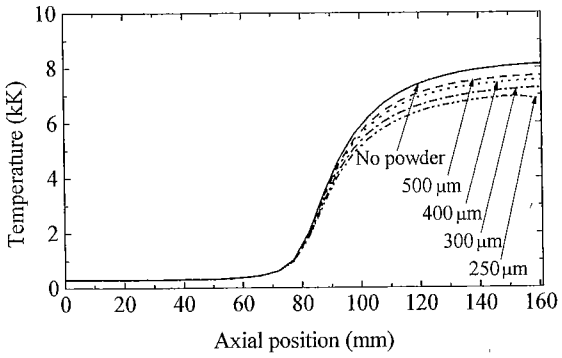

Fig. 10. Plasma temperature profiles along torch central axis

deviating distance obviously increases as a decrease in particle size.

The influence of powder size on individual particle heating from plasma can be clearly observed from particle temperature history shown in Fig. 9. For the particle injected at $r = 1.5$ mm, the exit temperature in case of diameter 250 μm is 856 K, while that in case of diameter

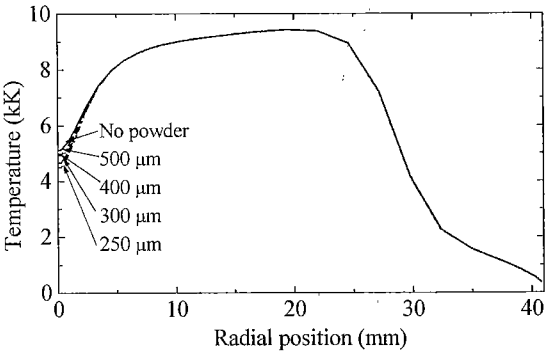

Fig. 11. Plasma temperature profiles along radial position at 10 mm below coil end

500 μm only reaches 482 K.

4.2 Plasma Temperature Fields Figures 10 and 11 show that the plasma temperature drops with a decrease in powder size. The smaller powder size decays plasma temperature much more. But this kind of influence is not so obvious as that of powder feed-rate as described as before.

5. Comparison of Predicted and Experimental Plasma Temperature

An experimental investigation about the effects of PTFE powder injection on Ar plasma was also carried out. The experimental conditions are listed in Table 4. Pressure 0.1 MPa and pure Ar sheath gas 100 l/min were fixed throughout the experiments. PTFE material powder of average diameter 410 μm was fed into the plasma with Ar carrier gas. The input power at the plate terminal of vacuum oscillator was fixed at 50 kW. Cosidering the conversion efficiency of vacuum tube oscillator is about 0.6, the given power to the plasma was estimated to be 30 kW. In the experiment, spectroscopic observations were first made for measuring the radiation intensity of Ar lines from thermal plasma. Then plasma temperature was estimated by using the two-line method of the spectral lines [11].

The spectral intensity of Ar I (703.0 nm) and Ar I (714.7 nm) at different radial positions, obtained by Abel inversion [12], were used for determining plasma radial temperature distribution at 10 mm below coil end. The results are shown in Fig. 12. Comparing this figure with Fig. 7, we can find that though the absolute value of temperature is different between the two figures, a similar temperatre decrease shape around torch center after injecting PTFE powder is clearly observed both in the calculation and in the experiment. The temperature difference between the experiment and computation can be considered from two sides. One is from the experiment. Some of the powder can be attached to torch wall when it is injected into the torch, which may bring the difficulty of spectroscopic observation and affect the precision of estimated temperature. Another reason from experiments is plasma state. Actual plasmas are not completely in LTE condition especially in radiation field. Excitation population of Ar may not always follow Boltzmann law, which results in a certain

Table 4. Experimental conditions

No	Sheath gas (Ar: l/min)	Carrier gas (Ar: l/min)	PTFE(g/min)
#1	100	6	0
#2	100	6	2

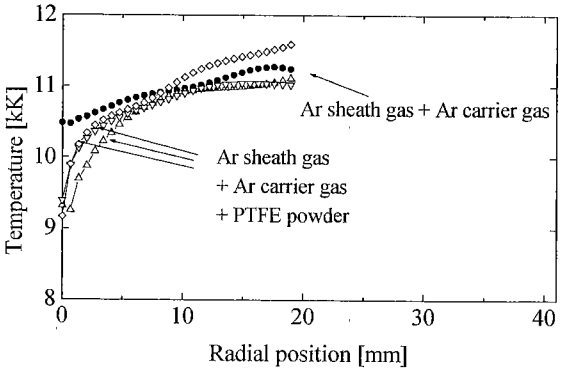

Fig. 12. Plasma radial temperature at 10 mm below coil end

error in temperature estimation. This occurs in not only a case with powder injection but also a case without powder injection. This is one of problems frequently faced in experiment. Other reason is from the computation. In the computation, some assumptions such as neglecting the particle-particle interaction and no internal heat transfer in the particles and LTE conditions were made.

6. Conclusions

A plasma-particle interaction model was developed, and used for the analysis of Ar induction plasma with PTFE powder injection. The computed results show that: (1) The injection of PTFE powder can cause a local cooling of Ar thermal plasma temperature field. (2) Increasing powder feed-rate decreases plasma temperature around torch center. (3) Smaller powder decays plasma temperature much more. (4) Particle trajectories and temperature history were related to many factors such as powder feed rate, particle size and injection location. Moreover, a similar decrease sharp of plasma temperature between experiment and simulation after PTFE powder injection is also found.

Acknowledgment

The authors would like to express a spectral thanks to Mr. T. Miwa (now at CHUBU Electric Power Company) for his cooperation in the experiment. This work is in part supported by a Grant-in Aid for Young Scientists (B)(No.15760195) in 2003.

(Manuscript received Feb. 28, 2003,
revised Sep. 11, 2003)

References

(1) Y. Tanaka and T. Sakuta: "Investigation of plasma-quenching efficiency of various gases using induction thermal plasma technique: effect of various gas injection on Ar thermal ICP", *J. Phys. D: Appl. Phys.*, Vol.35, pp.2149–2158 (2002)

(2) Y. Tanaka and T. Sakuta: "Stable operation region and dynamic behavior of pulse modulated Ar thermal plasma with different molecular gases", *T. IEE Japan*, Vol.123-A, No.5, pp.469–478 (2002-5)

(3) Y. Tanaka and T. Sakuta: "Plasma quenching effect of different environmentally benign gases at atmospheric pressure using ICTP technique", *T. IEE Japan*, Vol.121-B, No.7, pp.837–844 (2001-7)

(4) C.T. Crowe, M.P. Sharma, and D.E. Stock: "The Particle-Source-In Cell (PSI-CELL) Model for Gas-Droplet Flows", *J. Fluids Eng.*, Vol.99, pp.325–332 (1977)

(5) M.I. Boulos: "Heating of powders in the fire ball of an induction plasma", *IEEE Trans. Plasma Sci.* Vol.PS-6, pp.93–106 (1978)

(6) P. Proulx, J. Mostaghimi, and M.I. Boulos: "Plasma-particle intection effects in induction plasma modeling under dense loading conditions", *Int. J. Heat Mass Transfer,* Vol.28 pp.1327–1336 (1985)

(7) P. Proulx, J. Mostaghimi, and M.I. Boulos: "Heating of powder in an R.f. Inductively Coupled Plasma under Dense Loading Conditions", *Plasma Chem. Plasma Process.*, Vol.7, pp.29–52 (1987)

(8) T. Takagi, K. Nanbu, Y. Matsumoto, and S. Kamiyama: Analysis of complex flow, pp.1–35, Tokyo University Press, Tokyo (1995)

(9) S.V. Patankar: Numerical heat transfer and fluid flow, pp.131–134, Hemisphere Publishing Corporation, New York (1980)

(10) M. Matsuoka and S. Arai: "Ablated mass caused by the arc in plastic tubes", *T. IEE Japan*, Vol.118-B, No.12, pp.1380–1385 (1998-12)

(11) T.S. Vacquie, A. Gleizes, and H. Kafrouni: "Measurements of electron density in a SF_6 arc plasma", *J. Phys. D: Appl. Phys.*, Vol.18, pp.2193–2205 (1985)

(12) T.B. Reed: "Induction plasma torch", *J. Appl. Phys.*, Vol.32, pp.821–824 (1961)

Chun Wang (Non-member) was born on March 19, 1963. He received his B.S. degree from Xian Jiaotong University, China, in 1981, and M.S. and Ph.D. degrees from Kanazawa University, Japan, in 2000 and 2003, respectively, in electrical and electronic engineering. He is now working at the Department of Electrical and Automatic Engineering, Nanchang University, China. His research interests are thermal plasma and its applications.

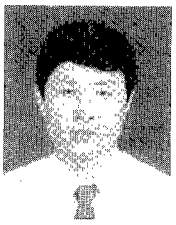

Yasumori Tanaka (Member) was born in Japan on November 19, 1970. He received the B.S, M.S. and Ph.D. degrees in electrical engineering from Nagoya University, Japan in 1993, 1995 and 1998 respectively. In April 1998 he was appointed Research Associate at Kanazawa University. He has been working as Associate Professor since August 2002 at the same university. His research interests include the arc interruption phenomena and thermal plasma applications.

Tadahiro Sakuta was born on January 3, 1950 and has passed away on January 26, 2003. He received the Ph.D. degree from Department of Electrical Engineering, Nagoya University, Japan in 1980. In April 1981 he was appointed a Research Associate at in the same Department. Since April 1988 he had been working as an Associate Professor and then as a Professor in the Department of Electrical and Electronic Engineering, Kanazawa University. His research intersets included the diagnosis and applications of high-pressure thermal plasmas including induction plasma and circuit breaker arcs.